Journal of Natural Medicines
https://doi.org/10.1007/s11418-021-01543-9

ORIGINAL PAPER

Cell death-inducing activities via Hsp inhibition of the sesquiterpenes isolated from *Valeriana fauriei*

Takahiro Matsumoto[1] · Takahiro Kitagawa[1] · Daisuke Imahori[1] · Hayato Yoshikawa[1] · Masaya Okayama[1] · Mayuka Kobayashi[1] · Naoto Kojima[1] · Masayuki Yamashita[1] · Tetsushi Watanabe[1]

Received: 26 May 2021 / Accepted: 25 June 2021

Abstract
Three new sesquiterpenes, valerianaterpenes I–III, and eight known compounds have been isolated from the methanol extract of the rhizomes and roots of *Valeriana fauriei*. The chemical structures of the three new sesquiterpenes were elucidated based on chemical and spectroscopic evidence. The absolute stereochemistry of valerianaterpene I was determined using X-ray crystallography. The cell death-inducing activity of isolated compounds alone or combination with Adriamycin (ADR) was observed by time-lapse cell imaging. Although the isolated compounds did not affect the number of mitotic entry cells and dead cells alone, kessyl glycol, kessyl glycol diacetate, and *iso*-teucladiol significantly increased the number of dead cells on ADR treated human cervical cancer cells. One of the mechanisms of cell death-inducing activity for the kessyl glycol acetate was suggested to be the inhibition of heat-shock protein 105 (Hsp105) expression level. This paper first deals with the naturally occurring compounds as Hsp105 inhibitor.

Keywords *Valeriana fauriei* · Valerianaterpene · X-ray crystallography · Time-lapse cell imaging · Heat-shock protein

Introduction

The genus *Valeriana* (Valerianaceae) contained more than 250 species of plants has been used as a mild sedative and sleep aid agent in Europe, Asia, and North America [1]. Among them, *Valeriana officinalis* is the official species in the European Pharmacopoeia and is commonly referred to as valerian [2]. From *V. officinalis*, iridoids [3] and sesquiterpenoids [4] including rare *N*-containing bisesquiterpenoid derivative [5] had been reported. On the other hand, *Valeriana fauriei* Briq., which belongs to the same genus plant as *V. officinalis* L. is abundant in the east Asia countries such as Japan and China, has been used for hundreds of years in folk medicine [6]. From *V. fauriei*, iridoids [7] and sesquiterpenoids [8] were reported same as *V. officinalis*. However, number of references about phytochemical research for *V. fauriei* is more limited than that of *V. officinalis*. In addition, there are quite few biological investigations for its characteristic constituents such as α-kessyl alcohol derivatives that have cyclized guaiane-type structures [9]. On our ongoing research program for the discovery of new cancer treatments and prevention agents [10–13], we pursued the isolation of characteristic sesquiterpenes enhancing the cytotoxicity of adriamycin (ADR) from *V. fauriei*.

ADR has been used as a potent chemotherapeutic drug for the treatment of several cancers [14]. ADR induces cell death via producing intercalates with base pairs of the DNA's double helix. Although this is effective in tumor therapy, the utilities of this compound are limited due to cardiotoxicity which is known to side effects [15]. Therefore, the compounds enhancing the cytotoxicity of ADR can reduce the dosage of ADR in tumor therapy to avoid the side effects should have the potency of new cancer treatment drugs. In addition, the anti-apoptotic function of heat-shock proteins (Hsps) had been suggested to be one of the major mechanisms on ADR registration of cancer cell [16]. Therefore, we evaluated inhibitory effects against the expression levels of several Hsp for cell death-induced compound.

✉ Takahiro Matsumoto
tmatsumo@mb.kyoto-phu.ac.jp

✉ Tetsushi Watanabe
watanabe@mb.kyoto-phu.ac.jp

[1] Kyoto Pharmaceutical University, Misasagi, Yamashina-ku, Kyoto 607-8412, Japan

Published online: 01 July 2021

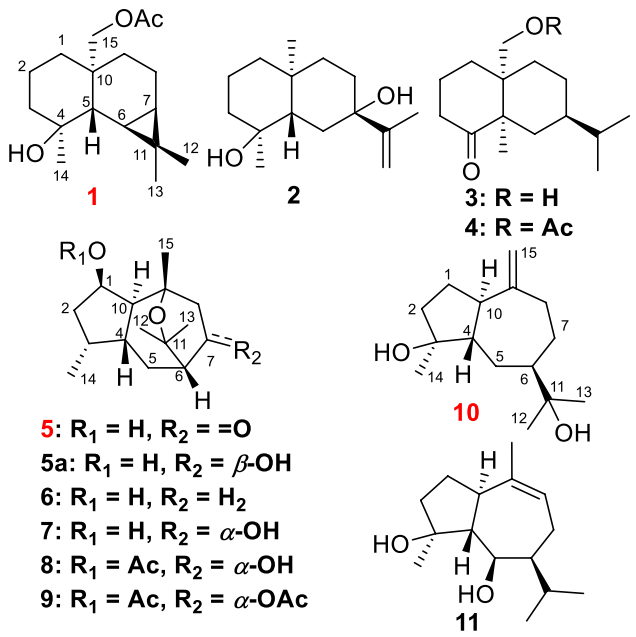

Fig. 1 The chemical structures of the isolated constituents (**1**–**11**) from *V. fauriei*

Results and discussion

The methanol extract of the rhizomes and roots of *V. fauriei* was partitioned in ethyl acetate–H_2O (1:1, v/v) to furnish an ethyl acetate-soluble fraction (3.1%) and aqueous layer (8.0%). The ethyl acetate-soluble fraction was subjected to normal- and reversed-phase silica gel column chromatography and repeated high-performance liquid chromatography (HPLC) to give three new compounds: valerianaterpene I (**1**, 0.0003%), II (**5**, 0.00095%), and III (**10**, 0.00031%), together with eight known compounds, 7β-hydroperoxy eudesma-11-en-4-ol (**2**, 0.00042%) [17], kanokonol (**3**, 0.0032%) [6], 15-acetoxyvaleranone (**4**, 0.018%) [18], *α*-kessyl alcohol (**6**, 0.00032%) [6], kessyl glycol (**7**, 0.0052%) [9], kessyl glycol acetate (**8**, 0.0091%) [9], kessyl glycol diacetate (**9**, 0.26%) [9], and *iso*-teucladiol (**11**, 0.26%) [19] (Fig. 1).

Valerianaterpene I (**1**) was isolated as colorless needle crystals (**1**) with positive optical rotations ($[\alpha]^{25}_{D}+8.8$ in MeOH). Its molecular formula ($C_{17}H_{28}O_3$) was determined using HRMS and ^{13}C NMR spectroscopy. A molecular ion peak was observed using EIMS for **1** (*m/z* 280 $[M]^+$). The ^1H and ^{13}C NMR ($CDCl_3$) spectra recorded for **1** (Table 1) show signals corresponding to a maaliol [20] moiety {three

Table 1 ^{13}C NMR (150 MHz) and ^1H NMR spectroscopic data (600 MHz) of valerianaterpenes I–III (**1**, **5**, and **10**) and **5a** recorded in $CDCl_3$

Position	**1**		**5**		**5a**		**10**	
	δC	δH (*J* in Hz)	δC	δH (*J* in Hz)	δC	δH (*J* in Hz)	δC	δH (*J* in Hz)
1	34.0	α 0.82 (m) β 1.64 (m)	73.5	4.17 (t-like, 4.1)	73.8	4.08 (m)	27.6	α 1.55 (m) β 1.75 (m)
2	19.9	1.47 (m)	43.2	α 1.33 (ddd, 8.9, 8.9, 15.1) β 2.03 (dd-like, 8.9, 15.1)	43.4	α 1.26 (m) β 1.29 (m)	40.6	α 1.77 (m) β 1.69 (m)
3	42.4	α 1.86 (m) β 1.39 (m)	30.7	2.28 (m)	30.4	2.22 (m)	81.1	
4	72.3		35.9	2.94 (m)	35.8	2.75 (m)	52.5	1.75 (m)
5	50.1	1.14 (d, 6.8)	26.5	α 1.58 (ddd, 7.6, 14.4, 14.4) β 2.12 (ddd, 7.6, 14.4, 14.4)	29.9	α 2.01 (m) β 1.99 (m)	25.5	1.67 (m)
6	19.2	0.50 (dd, 6.8, 9.6)	54.8	2.33 (d-like, 7.6)	46.5	1.67 (d-like, 6.0)	47.4	1.75 (m)
7	19.6	0.70 (t-like, 8.2)	213.0		73.1	4.06 (m)	27.0	α 1.28 (m) β 1.87 (m)
8	15.5	α 1.73 (m) β 1.53 (m)	52.2	α 2.36 (d, 18.5) β 2.67 (d, 18.5)	45.5	α 2.16 (dd, 9.6, 13.8) β 1.87 (dd, 8.4, 13.8)	37.9	α 2.04 (m) β 2.54 (ddd, 2.8, 6.9, 13.7)
9	34.5	α 1.64 (m) β 0.61 (m)	74.3		72.5		153.3	
10	36.7		55.4	1.43 (dd, 3.2, 13.6)	53.9	1.50 (m)	48.2	2.20 (dd, 8.0, 17.6)
11	18.5		75.5		75.8		74.2	
12	15.5	0.97 (s)	27.3	1.54 (s)	28.8	1.31 (s)	27.2	1.19 (s)
13	29.1	1.04 (s)	33.0	1.23 (s)	32.3	1.40 (s)	26.7	1.17 (s)
14	23.8	1.26 (s)	17.6	0.76 (d, 6.8)	18.1	0.79 (d, 7.2)	23.8	1.21 (s)
15	63.3	4.06 (d, 13.0) 4.27 (d, 13.0)	27.0	1.42 (s)	27.7	1.44 (s)	106.4	4.69 (br-s)
OAc	171.5							
	21.0	2.04 (s)						

methyl groups [δ_H0.97 (s, H-12), 1.04 (s, H-13), and 1.26 (s, H-14)], a methylene bearing oxygen function group [δ_H 4.06 (d, J = 13.0, H-15) and 4.27 (d, J = 13.0, H-15)], five methylenes [δ_C 34.0 (C-1), 19.9 (C-2), 42.4 (C-3), 15.5 (C-8), and 34.5 (C-9)], a methyne [δ_H 1.14 (d, J = 6.8, H-5), a quaternary carbon bearing oxygen function group [δ_C 72.3 (C-4)], and a quaternary carbon [δ_C 36.7 (C-10)]} together with an acetyl group [δ_C 171.5 (O*C*OCH$_3$) and 21.0 (OCO*C*H$_3$)]. The positions of the acyl group described above were determined based on the DQF COSY and HMBC spectra shown in Fig. 2. Namely, the long-range correlations were observed between H-5/C-15 and H-15/C-1, 9, 10, and O*C*OCH$_3$ suggested the acyl group was attached at C-15 (Fig. 2). Fortunately, crystals of **1** were obtained from MeOH–H_2O and X-ray crystallography used to determine the absolute stereochemistry of **1** (Fig. 3). Namely, the absolute stereochemistry was determined to be 4*R*,5*S*,6*R*,7*R*,10*R* using the Flack parameter [absolute structure parameter = 0.05(9)]. The NOESY spectra suggested above configuration same as X-ray crystallography data. Based on this evidence, the chemical structure of valerianaterpene I (**1**) was determined and shown in Fig. 1.

Valerianaterpene II (**5**) was isolated as a white amorphous powder with negative optical rotation ($[\alpha]^{25}_D$ -47.8 in MeOH). The molecular formula ($C_{15}H_{24}O_3$) was determined using HRMS and ^{13}C NMR spectroscopy. The ^{1}H and ^{13}C NMR ($CDCl_3$) spectra recorded for **5** (Table 1)

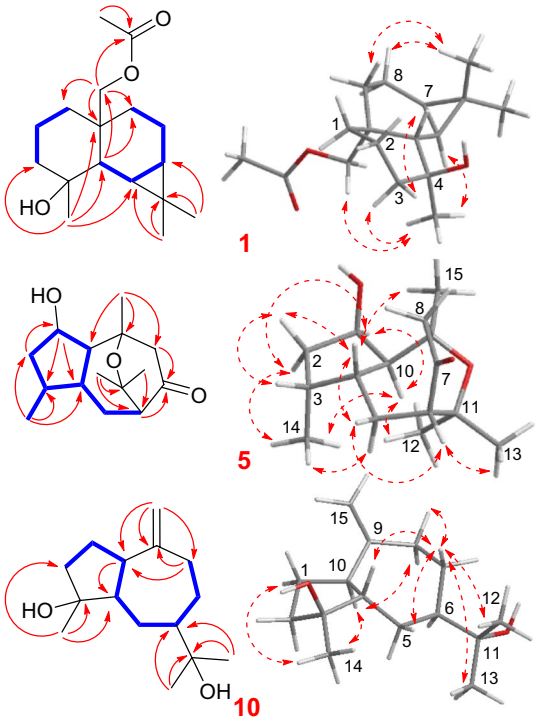

Fig. 2 Important 2D-NMR correlations of new constituents (**1**, **5**, and **10**)

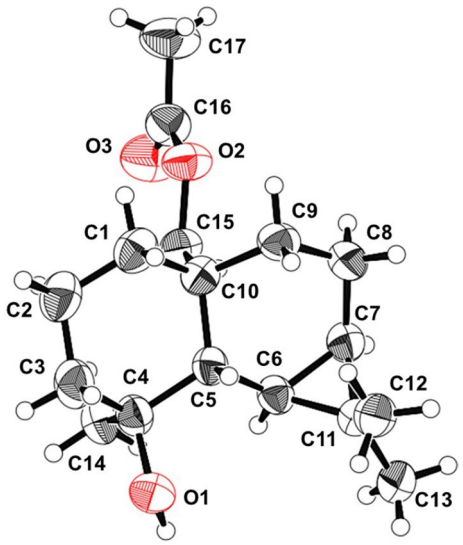

Fig. 3 ORTEP structure of valerianaterpene I (**1**)

show signals similar to kessyl glycol (**7**) including four methyl groups [δ_H 1.54 (s, H-12), 1.23 (s, H-13), 0.76 (d, J = 6.8, H-14), and 1.42 (s, H-15)], and two quaternary carbons bearing oxygen function group [δ_C74.3 (C-9) and 75.5 (C-11)]. The difference of **5** from **7** was the disappearance of a methine bearing oxygen function group at C-7 position and appearance of a carbonyl group. The position of carbonyl group described above was determined as C-7 from HMBC correlations between H-8/C-7 and H-6/C-7 (Fig. 2). NOESY cross-peaks corresponding to H-1/H-10, H-1/H-2α, H-10/H-12, and H-2α/H-14 suggested that H-1, H-2α, H-10, H-12, H-13, and H-14 were located on same side. In addition, NOESY cross-peaks corresponding to H-2β/H-3, H-2 β/H-4, H-4/H-5β, H-5β/H-6, H-4/H-15 suggested that H-2β, H-3, H-4, H-5β, H-6, and H-15 were located on same side. Therefore, the relative structure of **5** was determined as 1*R**,3*R**,4*R**,6*R**,9*S**,10*S**. Finally, the absolute stereochemistry of **5** was determined as 1*R*,3*R*,4*R*,6*R*,9*S*,10*S* from derivatization to kessyl glycol (**7**). Namely, reduction of **3** using $NaBH_4$ obtained **7** together with **5a**. Synthesized **7** was identified via ^{1}H NMR, MS, and optical rotation suggested absolute stereochemistry of **5** at C-1, 3, 4, 6, 9, and 10 were same as **7** [21]. Because of all this evidence, the chemical structure of valerianaterpene II (**5**) was determined and shown in Fig. 1. This compound may have been isolated as kessan 2-hydroxy-8-one, however, its chemical structure especially absolute stereochemistry has not been described in previous report [22, 23].

Valerianaterpene III (**10**) was isolated as a white amorphous powder with positive optical rotation ($[\alpha]^{25}_D$ + 17.8 in MeOH). The molecular formula ($C_{15}H_{26}O_2$) was determined using HRMS and ^{13}C NMR spectroscopy. The ^{1}H and ^{13}C NMR ($CDCl_3$) spectra corresponding to three methyl groups

[δ_H1.19 (s, H-12), 1.17 (s, H-13), and 1.21 (s, H-14)], two quaternary carbons bearing oxygen function group [δ_C81.1 (C-3) and 74.2 (C-11)], and two olefinic carbons [δ_C153.3 (C-9) and 106.4 (C-15)] were similar but different to that of pleocarpenene (3*R*,4*R*,6*R*,10*R*) [24] and diastereomer of pleocarpenene (3*R*,4*R*,6*R*,10*S*) [25]. Therefore, the chemical structure of **10** was assumed to be diastereomer of above described two compounds. The relative stereo structure of **10** was determined via NOESY spectra. Namely, cross-peaks corresponding to H-1α/H-14, H-10/H-8α, and H-10/H-14 suggested that H-1α, H-8α, H-10, and H-14 were located on same side. In addition, NOESY cross-peaks corresponding to H-4/H-7 β, H-5 β/7 β, H-7 β/H-8 β, H-7 β/H-12, and H-7 β/H-13 suggested that H-4, H-5 β, H-7 β, H-8 β, H-11, H-12 and H-13 were located on same side. Therefore, the relative structure of **10** was determined as 3*R**,4*S**,6*S**,10*R**. Finally, the absolute stereochemistry of **10** was deduced as 3*R*,4*S*,6*S*,10*R* from the other isolated guaiane-type sesquiterpenes and positive optical rotation ($[\alpha]^{25}_D + 15.1$ in $CHCl_3$) that was same tendency with that of **7** ($[\alpha]^{25}_D + 6.7$ in MeOH, recorded in this study) and known compound teucladiol ($[\alpha]^{25}_D + 2.1$ in $CHCl_3$, data from literature) [26]. Because of all this evidence, the chemical structure of valerianaterpene III (**10**) was determined and shown in Fig. 1.

ADR inhibits cell proliferation through induction of G2/M cell cycle arrest. Previous study suggested that the cell cycle arrest was induced via DNA damage; however, low concentrations of ADR (0.1–1.0 μg/ml) does not induce cell death [16]. Therefore, the compounds increase the number of dead cells on low concentration ADR treatment cells may be able to reduce the dosage of ADR in tumor therapy to avoid the side effects. We evaluated the cell death-inducing activities of isolated compounds on HeLa cells by 24 h using time-lapse imaging analysis. In this study, we counted the number of mitotic entry cells and dead cells under treatment of low concentration ADR (1.0 μg/ml), test compounds (**1**–**11**) (60 μM), and combination of test compounds (60 μM) with ADR (1.0 μg/ml). As the results, ADR significantly reduced the mitotic entry cells but did not increase the dead cells same as previous report [27]. All isolated compounds (**1**–**11**, 60 μM) treatment did not affect the number of the dead cells and the mitotic entry cells (Fig. 4A). However, combination treatment of **7**, **9**, and **11** with ADR significantly increased the dead cells compared to those of ADR treated cells (Fig. 4B). Above results suggested that **7**, **9**, and **11** may have the potency for cancer treatment agents without show side effects (Fig. 5).

Hsp105 is a molecular chaperone, and it was reported to suppress ADR-induced cell death via anti-apoptotic functions [16]. Because Hsp105 is overexpressed in several kinds of tumor, inhibition of Hsp105 have been suggested to be a target for cancer chemotherapy [26]. Previously, only one small molecule organic compound, KNK437

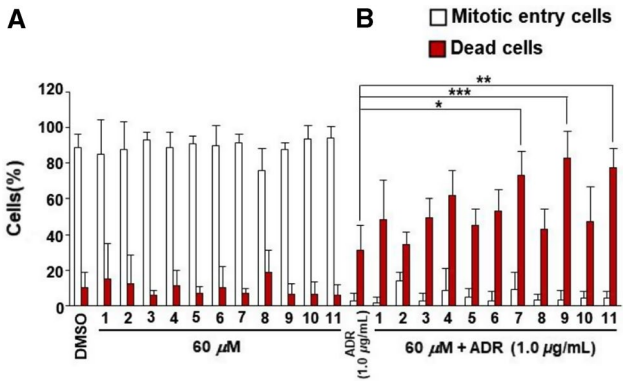

Fig. 4 Effects of the isolated compounds (**1**–**11**) on cell proliferation and cell death. (A) HeLa cells were treated with 60 μM indicated compounds, (B) ADR (1.0 μg/ml) or combination of them for 24 h. The number of mitotic entry cells and dead cells was counted during time-lapse imaging. The percentages of mitotic entry cells or dead cells are reported as means ± SD of triplicate. Statistical significance was analyzed using the Tukey–Kramer test (*$P < 0.05$, **$P < 0.01$, ***$P < 0.001$ compared with ADR (1.0 μg/ml)-treated cells)

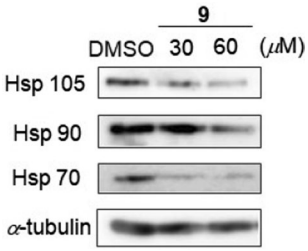

Fig. 5 The expression levels Hsp105, 90, and 70 on HeLa cell treated with **9** for 24 h

that have benzylidene lactam structure was reported as Hsp105 inhibitor [28, 29]. Hsp70 is also have anti-apoptotic functions and it is induced by Hsp105 [30]. On the other hand, inhibition of Hsp90 was reported to induce other Hsps such as Hsp70 [31]; therefore, the compounds inhibit Hsp105 and 70 without affect Hsp90 should be new cancer treatment agents. The HeLa cell is the one of the Hsp105 overexpression cancer cell line and siRNA-mediated knockdown of Hsp105 enhances ADR-induced cell death [16]. Among the isolated compounds in this study, **9** showed strongest cell death-inducing activity on ADR treatment cell; therefore, we evaluated expression levels of Hsp105, 90, and 70 in **9** treated HeLa cell using western blotting analysis. As the result, **9** inhibited the expression of Hsp105 and 70 without affects the Hsp90 at 30 μm. The expression level of Hsp90 was weakly suppressed by 60 μm treatment of **9**. Based on above results, we concluded that **9** is able to enhance the effects of previous cancer treatment agents such as ADR via inhibition of Hsp105 expression. In the vest of our knowledge, this

is the first report deals with the naturally occurring compounds as Hsp105 inhibitor.

Experimental section

General experimental procedures

Specific rotations were obtained on a JASCO P-2200 digital polarimeter (l = 5 cm). EIMS and HREIMS were recorded on JEOL JMS-GCMATE mass spectrometer. ^{1}H NMR spectroscopy was recorded on JEOL ECS400 (400 MHz) and JNM-ECA 600 (600 MHz) spectrometers. ^{13}C NMR spectroscopy was recorded on a JNM-ECA 600 (150 MHz) spectrometer. 2D-NMR experiments were carried out on a JEOL JNM-ECA 600 (600 MHz) spectrometer.

Normal-phase silica gel column chromatography was carried out using Silica gel 60 (Kanto Chemical Co., Inc. 63–210 mesh) and reversed-phase silica gel column chromatography was carried out on C_{18}-OPN (Nakalai Tesque Co., Inc. 140 μm). Thin-layer chromatography (TLC) was performed using TLC plates pre-coated with $60F_{254}$ silica gel (Merck, 0.25 mm; ordinary phase) and RP-18 F_{254S} silica gel (Merck, 0.25 mm; reversed-phase). Reversed-phase high-performance TLC was carried out using TLC plates pre-coated with RP-18 WF_{254S} silica gel (Merck, 0.25 mm). HPLC was performed using a Shimadzu SPD-M10Avp UV–vis detector. COSMOSIL 5C18-MS-II (250 × 4.6 mm i.d., 250 × 10 mm i.d. and 250 × 20 mm i.d.) and YMC-Triart PFP (250 × 4.6 mm i.d. and 250 × 10 mm i.d.) columns were used for analytical and preparative purposes.

Plant material

The rhizomes and roots of *V. fauriei* distributed in the Hokkaido of Japan were purchased from Tochimoto Tenkaido (Osaka prefecture, Japan) in August 2020.

Extraction and isolation

The rhizomes and roots of *V. fauriei* (6 kg) were extracted three times with methanol under reflux for 3 h. Evaporation of the solvent provided a methanol extract (1150 g). The methanol extract was partitioned into ethyl acetate–water (1:1, v/v) to furnish an ethyl acetate-soluble fraction (190.1 g, 3.1%) and water-soluble fraction (959.9 g, 8.0%). The ethyl acetate-soluble fraction was subjected to normal-phase silica gel column chromatography [*n*-hexane–$CHCl_3$ (1:1 → 0:1, v/v) → $CHCl_3$–MeOH (50:1 → 20:1 → 10:1 → 5 :1 → 1:1, v/v)] to give ten fractions. Fraction 4 (30.1 g) was separated using reversed-phase silica gel column chromatography to give nine fractions. Fraction 4–2 (1015.2 mg) was purified using HPLC {H_2O–CH_3CN (70:30, v/v)} to give **5** (18.0 mg). From the fraction 4–3 (6785.7 mg), **9** (4.9 g) was obtained by recrystallization (*n*-hexane–$CHCl_3$). Fraction 4–4 (2759.2 mg) was purified using HPLC {H_2O–CH_3CN (40:60, v/v)} to give **1** (5.7 mg), **3** (61.1 mg), **4** (338.7 mg), **6** (6.1 mg), **8** (173.0 mg), and **11** (5.2 mg). Fraction 5 (2.98 g) was separated using reversed-phase silica gel column chromatography to give five fractions. Fraction 5–1 (477.8 mg) was purified using HPLC {H_2O–CH_3CN–CH_3COOH (80:20:0.3, v/v/v)} to give **7** (98.2 mg). Fraction 5–3 (852.5 mg) was purified using HPLC {H_2O–CH_3CN (65:35, v/v)} to give **2** (8.9 mg) and **10** (5.8 mg).

Valerianaterpene I (*1*)

Colorless needle crystals; $[\alpha]^{25}_{D}$ + 8.8 (*c* 0.14, MeOH); ^{1}H NMR ($CDCl_3$, 600 MHz) and ^{13}C NMR ($CDCl_3$, 150 MHz), see Table 1; EIMS *m/z* 280 $[M]^+$; HREIMS *m/z* 280.2036 $[M]^+$ (calcd for $C_{17}H_{28}O_3$, 280.2039).

X-ray diffraction analysis of valerianaterpene I (*1*)

A colorless needle crystal of $C_{17}H_{28}O_3$ with approximate dimensions of 0.200 × 0.100 × 0.050 mm was mounted on a Dual-Thickness MicroMouunt™. All measurements were performed using a Rigaku R-AXIS RAPID II diffractometer with graphite monochromated Cu-Kα radiation. The crystal-to-detector distance was 127.40 mm. MW 280.41, monoclinic, space group $P2_12_12_1$ (#19), a = 6.5826(3) Å, b = 14.2197(7) Å, c = 17.2972(8) Å, V = 1619.07(13) $Å^3$, Z = 4, D_{calcd} = 1.150 g/cm^3, μ(Cu-Kα) = 6.087 cm^{-1}, F(000) = 616.00, No. of reflections measured: Total, 17,862; unique, 2927 (R_{int} = 0.0434); Flack parameter: 0.05(9). Further crystallographic data regarding the compound structure can be found in the supporting information. Crystallographic data for **1** have been deposited with the Cambridge Crystallographic Data Centre (deposition number CCDC 2084835).

Valerianaterpene II (*5*)

White amorphous powder; $[\alpha]^{25}_{D}$ -47.8 (*c* 0.37, MeOH); ^{1}H NMR ($CDCl_3$, 600 MHz) and ^{13}C NMR ($CDCl_3$, 150 MHz), see Table 1; EIMS *m/z* 252 $[M]^+$; HREIMS *m/z* 252.1725 $[M]^+$ (calcd for $C_{15}H_{24}O_3$, 252.1726).

$NaBH_4$ reduction of 5

To a solution of **5** (5.0 mg, 0.02 mmol) in MeOH (5 mL) was added $NaBH_4$ (5 mg, 0.13 mmol) and the mixture was stirred for 0.5 h at 0 °C. Saturated aqueous $NaHCO_3$ was added, and the solution was extracted by CH_2Cl_2. The residue was purified using HPLC {H_2O–CH_3CN (65:35, v/v)} to give **7** (1.0 mg, 0.004 mmol, 19.8%) and **5a** (0.6 mg, 0.0024 mmol, 11.9%).

Data for *7* derived from *5*

White amorphous powder; $[\alpha]^{25}_{D}$ -24.8 (*c* 0.05, MeOH); ^{1}H NMR ($CDCl_3$, 600 MHz) and ^{13}C NMR ($CDCl_3$, 150 MHz) were identical with literature [9]; EIMS *m/z* 254 $[M]^+$; HREIMS *m/z* 254.1886 $[M]^+$ (calcd for $C_{15}H_{26}O_3$, 254.1882).

Data for *5a* derived from *5*

White amorphous powder; $[\alpha]^{25}_{D}$ -31.7 (*c* 0.37, MeOH); ^{1}H ($CDCl_3$, 600 MHz) and ^{13}C NMR ($CDCl_3$, 150 MHz), see Table 1; EIMS *m/z* 254 $[M]^+$; HREIMS *m/z* 254.1882 $[M]^+$ (calcd for $C_{15}H_{26}O_3$, 254.1882).

Valerianaterpene III (*10*)

White amorphous powder; $[\alpha]^{25}_{D}$ + 17.8 (*c* 0.14, MeOH); ^{1}H NMR ($CDCl_3$, 600 MHz) and ^{13}C NMR ($CDCl_3$, 150 MHz), see Table 1; EIMS *m/z* 238 $[M]^+$; HREIMS *m/z* 238.1930 (calcd for $C_{15}H_{26}O_2$ $[M]^+$, 238.1933).

Cells

Human cervical carcinoma (HeLa) cells were maintained in Dulbecco's modified Eagle's medium (DMEM) with low glucose (Wako Pure Chemical Industries, Osaka, Japan) supplemented with 5% fetal bovine serum (Merck, Darmstadt, Germany) under a 5% CO_2 atmosphere at 37 ℃.

Time-lapse imaging

Time-lapse imaging was performed on an Operetta high-content imaging system (PerkinElmer, Waltham, MA) as described previously [13]. Briefly, the cells were cultured in a flat-bottomed 24-well plate (Coaster 3526; Corning) to reach 70–80% confluence. The cells were then treated with test compounds or Adriamycin just prior to the time-lapse cell imaging. The images were captured at 10 min intervals for 24 h under a 5% CO_2 atmosphere at 37 ℃.

Statistical analysis

Statistical analyses were performed using GraphPad Prism 8.21 software. The statistical analysis was conducted using one-way analysis of variance (ANOVA) followed by a Tukey–Kramer test to analyze the differences between the treatment groups. The significance level used for statistical analysis with two-tailed testing was 5%.

Western blotting analysis

HeLa cells (1.0×10^5 cells) were seeded into 35-mm dishes. After 24 h of incubation, the cells were treated with various concentrations of compounds for 24 h. Cells were lysed with sodium dodecyl sulfate (SDS)-sample buffer (2% SDS, 10% glycerol, 5% 2-mercaptoethanol, 62.5 mM Tris-HCl [pH 6.8], and 0.0125% bromophenol blue) and boiled at 100 ℃ for 5 min. Proteins were separated by SDS-PAGE and transferred onto polyvinylidene difluoride membranes (Pall Corporation, Port Washington, NY). Blots were incubated with Blocking One (Nacalai Tesque), and sequentially incubated with appropriate primary and horseradish peroxidase (HRP)-conjugated secondary antibodies that were diluted with Tris-buffered saline containing 0.1% Tween 20 and 5% Blocking One. Chemiluminescence was detected with an image analyzer LAS-4000 mini system (Fujifilm, Tokyo, Japan) using Clarity Western ECL Substrate (Bio-Rad, Hercules, CA). Antibodies used in this study were as follows: mouse monoclonal anti-Hsp105 (1:1000–2000; E5Q6W, Santa Cruz Biotechnology, Dallas, TX, USA), anti-Hsp90 (1:2000; clone AC88, Enzo Life Sciences, Farming dale, NY, USA), anti-Hsp70 (1:2000; clone C92F3A-5, Enzo Life Sciences), and anti-α-tubulin (1:2000; clone DM1A, Sigma-Aldrich, St. Louis, MO, USA) antibodies. HRP-conjugated goat anti-mouse IgG (1:4000; 712–035-151) were purchased form Jackson ImmunoResearch Laboratories Inc. (West Grove, PA, USA).

Supporting information

The ^{1}H and ^{13}C NMR spectra for **1**, **5**, and **10** and crystallographic data for **1** are available in the supporting information.

Supplementary Information The online version contains supplementary material available at https://doi.org/10.1007/s11418-021-01543-9.

Acknowledgements This work was supported by JSPS KAKENHI Grant Numbers 20H03397 and 20J14567.

References

1. Wang P-C, Ran X-H, Luo H-R, Hu J-M, Chen R, Ma Q-Y, Dai H-F, Liu Y-Q, Xie M-J, Zhou J, Zhao Y-X (2011) Volvalerelactones A and B, two new sesquiterpenoid lactones with an unprecedented skeleton from *Valeriana officinalis* var. *latifolia*. Org Lett 13:3036–3039
2. Piccinelli A-L, Arana S, Caceres A, di Villa Bianca Rd, Sorrentino R, Rastrelli L, (2004) New lignans from the roots of *Valeriana*

prionophylla with antioxidative and vasorelaxant activities. J Nat Prod 67:1135–1140
3. Lee D-H, Park S-H, Huh Y-H, Kim M-J, Seo H-D, Ha T-Y, Ahn J, Jang Y-J, Jung C-H (2020) Iridoids of *Valeriana fauriei* contribute to alleviating hepatic steatosis in obese mice by lipophagy. Biomed Pharmacother 125:109950
4. Liu X-G, Gao P-Y, Wang G-S, Song S-J, Li L-Z, Li X, Yao X-S, Zhang Z-X (2012) In vivo antidepressant activity of sesquiterpenes from the roots of *Valeriana fauriei* Briq. Fitoterapia 83:599–603
5. Wang P-C, Ran X-H, Luo H-R, Ma Q-Y, Zhou J, Hu J-M, Zhao Y-X (2016) Volvalerine A, an unprecedented N-containing sesquiterpenoid dimer derivative from *Valeriana officinalis* var. *latifolia*. Fitoterapia 109:174–178
6. Oshima Y, Matsuoka S, Ohizumi Y (1995) Antidepressant principles of *Valeriana fauriei* roots. Chem Pharm Bull 43:169–170
7. Guo Y, Xu J, Li Y, Watanabe R, Oshima Y, Yamakuni T, Ohizumi Y (2006) Iridoids and sesquiterpenoids with NGF-potentiating activity from the rhizomes and roots of *Valeriana fauriei*. Chem Pharm Bull 54:123–125
8. Liu X-G, Zhang W-C, Gao P-Y, Wang G-S, Li L-Z, Song S-J, Zhang X, Yao X-S, Liu K, Zhang Z-X (2013) Two new sesquiterpenes from the roots of *Valeriana fauriei* Briq. Helv Chim Acta 96:651–655
9. Nishiya K, Kimura T, Takeya K, Itokawa H (1992) Sesquiterpenoids and iridoid glycosides from *Valeriana faueriei*. Phytochemistry 31:3511–3514
10. Matsumoto T, Kitagawa T, Imahori D, Matsuzaki A, Saito Y, Ohta T, Yoshida T, Nakayama Y, Ashihara E, Watanabe T (2021) Linderapyrone: A Wnt signal inhibitor isolated from *Lindera umbellata*. Bioorg Med Chem Lett 45:128161
11. Matsumoto T, Kitagawa T, Teo S, Anai Y, Ikeda R, Imahori D, Ahmad HSB, Watanabe T (2018) Structures and antimutagenic effects of onoceranoid-type triterpenoids from the leaves of *Lansium domesticum*. J Nat Prod 81:2187–2194
12. Matsumoto T, Imahori D, Saito Y, Zhang W, Ohta T, Yoshida T, Nakayama Y, Ashihara E, Watanabe T (2020) Cytotoxic activities of sesquiterpenoids from the aerial parts of *Petasites japonicus* against cancer stem cells. J Nat Med 74:689–701
13. Matsumoto T, Imahori D, Achiwa K, Saito Y, Ohta T, Yoshida T, Kojima N, Yamashita M, Nakayama Y, Watanabe T (2020) Chemical structures and cytotoxic activities of the constituents isolated from *Hibiscus tiliaceus*. Fitoterapia 142:104524
14. Damiani RM, Moura DJ, Viau CM, Caceres RA, Henriques JAP, Saffi J (2016) Pathways of cardiac toxicity: comparison between chemotherapeutic drugs doxorubicin and mitoxantrone. Arch Toxicol 90:2063–2076
15. Cheung KG, Cole LK, Xiang B, Chen K, Ma X, Myal Y, Hatch GM, Tong Q, Dolinsky VW (2015) Sirtuin-3 (SIRT3) protein attenuates doxorubicin-induced oxidative stress and improves mitochondrial respiration in H9c2 cardiomyocytes. J Biol Chem 290:10981–10993
16. Yamane T, Saito Y, Teshima H, Hagino M, Kakihana A, Sato S, Shimada M, Kato Y, Kuga T, Yamagishi N, Nakayama Y (2019) Hsp105α suppresses Adriamycin-induced cell death via nuclear localization signal-dependent nuclear accumulation. J Cell Biochem 120:17951–17962
17. Lee S-O, Choi S-Z, Choi S-U, Kim G-H, Kim Y-C, Lee K-R (2006) Cytotoxic terpene hydroperoxides from the aerial parts of *Aster spathulifofius*. Arc Pharm Res 29:845–848
18. Fokialakis N, Magiatis P, Mitaku S (2002) Essential oil constituents of *Valeriana italica* and *Valeriana tuberosa*. Stereochemical and conformational study of 15-acetoxyvaleranone. Z Naturforsch C 57:791–796
19. Dowling M-S, Vanderwal C-D (2010) Ring-closing metathesis of allylsilanes as a flexible strategy toward cyclic terpenes. short syntheses of teucladiol, isoteucladiol, poitediol, and dactylol and an attempted synthesis of caryophyllene. J Org Chem 75:6908–6922
20. Buchi G, White D-M (1957) The ring fission of cyclopropanes: the constitution of maaliol. J Am Chem Soc 79:750–751
21. Ito S, Kodama M, Nozoe T (1967) Structure and absolute configuration of α-kessyl alcohol and kessyl glycol. Tetrahedron lett 23:553–563
22. Takamura K, Kawaguchi M, Nabata H (1975) The preparation and pharmacological screening of kessoglycol derivative. Yakugaku Zasshi 95:1198–1204
23. Takamura K, Nabata H, Kawaguchi M (1975) The pharmaceutical action on the kessoglycol 8-monoacetate. Yakugaku Zasshi 95:1205–1209
24. Williams M-J, Deak H-L, Snapper M-L (2007) Intramolecular cyclobutadiene cycloaddition/cyclopropanation/thermal fragmentation: An effective strategy for the asymmetric synthesis of pleocarpenene and pleocarpenone. J Am Chem Soc 129:486–487
25. Silva M, Wiesenfeld A, Sammes P-G, Tyler T-W (1977) New sesquiterpenes from *Pleocarpus revolutus*. Phytochemistry 16:379–385
26. Aguilar-Guadarrama A-B, Rios M-Y (2004) Three new sesquiterpenes from *Croton arboreous*. J Nat Prod 67:914–917
27. Kitagawa T, Matsumoto T, Imahori D, Kobayashi M, Okayama M, Ohta T, Yoshida T, Watanabe T (2021) Limonoids isolated from the *Fortunella crassifolia* and the *Citrus junos* with their cell death inducing activity on Adriamycin treated cancer cell. J Nat Med, in press
28. Kai M, Nakatsura T, Egami H, Senju S, Nishimura Y, Ogawa M (2003) Heat shock protein 105 is overexpressed in a variety of human tumors. Oncol Rep 10:1777–1782
29. Yang S, Ren X, Liang Y, Yan Y, Zhou Y, Hu J, Wang Z, Song F, Wang F, Liao W, Liao W, Ding Y, Liang L (2020) KNK437 restricts the growth and metastasis of colorectal cancer via targeting DNAJA1/CDC45 axis. Oncogene 39:249–261
30. Saito Y, Yamagishi N, Hatayama T (2008) Nuclear localization mechanism of Hsp105β and its possible function in mammalian cells. J Biochem 145:185–191
31. Griffin T-M, Valdez T-V, Mestril R (2003) Radicicol activates heat shock protein expression and cardioprotection in neonatal rat cardiomyocytes. Amer J Physiol Heart Circ Phy 287:1081–1088